



Published in final edited form as:

J Mater Chem B Mater Biol Med. 2015 December 28; 3(48): 9277–9284. doi:10.1039/C5TB02067K.

A simple method for the synthesis of porous polymeric vesicles and their application as MR contrast agents

Lesan Yan, Elizabeth Higbee, Andrew Tsourkas, and Zhiliang Cheng

Department of Bioengineering, University of Pennsylvania, Philadelphia, PA 19104, USA

Zhiliang Cheng: zcheng@seas.upenn.edu

Abstract

Because of their low membrane permeability the use of polymeric vesicles in certain drug delivery and molecular imaging applications and as bioreactors is less than ideal. Here, we report a simple method to prepare porous polymeric vesicles that possess high membrane permeability.

Specifically, porous vesicles were produced from the aqueous assembly of the diblock copolymer PEG-PBD, and the triblock copolymer PEG-PPO-PEG. It was found that PEG-PPO-PEG-doped polymersomes exhibited improved membrane permeability to molecules less than 5 kDa. Further, these porous vesicles retained molecules > 10 kDa within their aqueous interiors with no significant leakage. To demonstrate its application, highly efficient magnetic resonance contrast agents were produced from porous polymersomes by encapsulating macromolecules labeled with gadolinium. Due to a fast water exchange rate with surrounding bulk water, these paramagnetic porous polymersomes exhibited higher r_1 relaxivity compared with Gd-encapsulated vesicles with no pores. Due to their simplicity, the porous polymersomes prepared with this method are expected to have additional useful applications.

1. Introduction

Polymeric vesicles, or polymersomes, are generated by self-assembling amphiphilic di- or tri-block copolymers in aqueous solvents. While having many of the properties of phospholipid liposomes, these polymeric vesicles exhibit enhanced mechanical and chemical stability, the ability to load larger quantities of hydrophilic and hydrophobic components, and a long blood circulation time. Furthermore, the use of synthetic polymers offers extensive possibilities to manipulate the membrane properties of the polymersomes including stability, fluidity, and intermembrane dynamics.¹ As a result of these characteristics, polymersomes have garnered a great deal of interest as nanoplatforms for a range of biomedical applications, including drug delivery,^{2–5} *in vivo* imaging,^{6–14} and for use as cell mimetics.^{15–17}

Due to their thicker membranes, the membrane permeability of polymersomes is 10 to 20 times lower than the value encountered for phospholipid liposomes. For instance, water

Correspondence to: Zhiliang Cheng, zcheng@seas.upenn.edu.

†Electronic Supplementary Information (ESI) available: Stability of porous vesicles, Cryo-TEM of porous vesicles, release and retention of vesicles prepared with 100 mol% PEG-PBD, pH sensitivity of vesicles prepared with 100 mol% PEG-PBD, relaxivity of Gd-GC-conjugates and cell viability of vesicles. See DOI: 10.1039/x0xx00000x

permeability is 15–150 $\mu\text{m/s}$ for liposomes, while it is only 0.7–10 $\mu\text{m/s}$ for polymersomes.¹⁸ The relative impermeability of the polymersome membrane can be problematic for numerous biomedical applications. For example, in order for polymersomes to be used as highly efficient magnetic resonance (MR) contrast agents, encapsulated gadolinium (Gd) should have access to freely diffusing bulk water surrounding the polymersome to maximize contrast. Unfortunately, polymersomes with encapsulated Gd have not been widely adopted as highly efficient MR contrast agents due to the detrimental effects of the slow water exchange rate through the vesicle bilayer on the relaxivity of encapsulated Gd.¹⁹ Similarly, in order for polymersomes to be used as bioreactors or artificial cells, they should allow specific external substances to pass into the aqueous interior and interact with encapsulated active molecules.²⁰

To date, a substantial amount of effort has been made in tuning polymersome membrane permeability. The most widely used methods include using external stimuli including pH,^{21–23} carbon dioxide,²⁴ temperature,²⁵ light,²⁶ magnetic field,²⁷ or ion channels.²⁸ For example, several groups have found that the addition of channels and carriers into polymersomes was able to improve membrane permeability.^{20, 29–31} However, in general, polymersome membranes are too thick and many naturally occurring transmembrane protein channels cannot span the entire membrane, decreasing the activity of the inserted channels.^{28, 32, 33} Another approach was recently developed by our group,³⁴ where a small amount of phospholipid was incorporated into crosslinkable polymersome membranes. Following crosslinking of the polymer, the phospholipid was extracted from the polymersome with surfactant, generating a highly porous outer membrane that allowed for the transport of small molecules across the membrane. However, this approach suffered from complicated synthesis. In addition, free-radical crosslinking could have an effect on the activity of encapsulated dyes, drugs or proteins, and thus potentially reduce the efficacy of diagnosis or therapy. Therefore, we sought to develop a simple method for preparing porous polymersomes that could overcome these limitations, including toxicity, complexity, and cost.

Poly(ethylene glycol)-*block*-poly(propylene oxide)-*block*-poly(ethylene glycol) (PEG-PPO-PEG) are a class of triblock copolymers consisting of hydrophilic PEG (poly(ethylene oxide)) and hydrophobic PPO (poly(propylene oxide)). These materials are readily available, nontoxic, low cost, and now used in a variety of applications as emulsifiers and drug delivery system.^{35, 36} Several studies have showed that PEG-PPO-PEG can be used to form vesicles.^{37–41} For example, Rodríguez-García et al showed that PEG-PPO-PEG (Pluronic L121) could form giant polymersomes with high membrane permeability to hydrophilic solutes.³⁹ Since PEG-PPO-PEG membrane was relatively soluble in water, these polymersomes had a low membrane rigidity and could only be stable in solution for several hours.^{36, 42} The poor stability of PEG-PPO-PEG vesicles greatly limits their applications. It is known that polymersomes made from classical diblock copolymer such as PEG-PBD have a rigid bilayer and an increased mechanical stability.^{1, 39, 43} However, the membrane permeability of these PEG-PBD polymersomes is significantly lower than the permeability of PEG-PPO-PEG vesicles.³⁹ In this work, we explore the preparation of polymersomes made from the mixture of PEG-PBD and PEG-PPO-PEG, which possess a more stable

bilayer with enhanced membrane permeability. Specifically, PEG-PPO-PEG triblock copolymers were incorporated into PEG-PBD based diblock copolymer, and nanometer-sized polymeric vesicles were formed via film-hydration and extrusion technique. The vesicles were first evaluated for their leakage and retention properties, then for their biomedical application as MR contrast agents.

2. Materials and methods

2.1. Materials

Poly(ethylene glycol) (600)-polybutadiene (1200) copolymer (denoted PEG-PBD) was purchased from Polymer Source (Dorval, Quebec, Canada). Glycol chitosan was purchased from Wako Chemicals (Richmond, VA). DTPA dianhydride, gadolinium (III) chloride, fluorescein isothiocyanate-dextran (FITC-dextran MW 59,000–77,000), tetramethylrhodamine isothiocyanate-Dextran (TRITC-dextran, MW 4400) and poly(ethylene glycol)-block-poly(propylene oxide)-block-poly(ethylene glycol) (PEG-PPO-PEG, MW 4400) were obtained from Sigma-Aldrich. Sulforhodamine B (SRB), tetramethylrhodamine-dextran (TRITC-dextran, 10,000 MW) and tetramethylrhodamine-dextran (TRITC-dextran, 40,000 MW) were obtained from Thermo Fisher Scientific Inc. All other chemicals were used as received. All of the buffer solutions were prepared with deionized water.

2.2. Synthesis of GC-DTPA-Gd

High-molecular-weight glycol chitosan was degraded as previously described.^{44, 45} Specifically, 10 g of ~600 kDa glycol chitosan was dissolved in 200 mL of 6 M HCl and heated to 80 °C for 2 h. Following incubation, the material was cooled on ice and immediately neutralized with solid sodium carbonate to terminate degradation. Excess base was removed by centrifugation, and diafiltration membranes (100, 50, 30, and 10 kDa MWCO) were used sequentially to desalt the material and discard any GC polymer greater than 30 kDa or less than 10 kDa. The fraction collected between 10–30 kDa was washed with water for three cycles using a 5000 MWCO membrane filter, and then vacuum-dried and used without any further purification.

A 120 mg portion of GC (MW: 10–30K) was dissolved in 5 mL of sodium bicarbonate buffer (0.1 M, pH 8.5) and reacted with 400 mg of DTPA dianhydride. The reaction solutions were maintained at pH 8.5 with NaOH over the reaction time of 15 h. The GC–DTPA was purified by centrifugal filter devices (Amicon Ultra-4, 10,000 MWCO, Millipore Corp.). The purified GC–DTPA conjugates were mixed with 100 mg of GdCl₃ in 0.1 M citrate buffer (pH 5.6) overnight at 42 °C. The unreacted Gd³⁺ was removed by centrifugal filter devices (Amicon Ultra-4, 10,000 MWCO, Millipore Corp.) while simultaneously changing the buffer to 10 mM HEPES buffer (pH 7.4). The purified GC–DTPA–Gd conjugates were used for vesicle encapsulation.

2.3. Preparation of Giant Vesicles

Giant polymer vesicles were prepared as previously described.³⁴ Stock solutions of PEG-PBD and PEG-PPO-PEG in chloroform were mixed in the following molar ratios: PEG-

PBD/ PEG-PPO-PEG (100:0), PEG-PBD/ PEG-PPO-PEG (90:10), and PEG-PBD/ PEG-PPO-PEG (75:25). In all cases, the total amount of PEG-PBD for each of the vesicle compositions was 1 mg. The solvent was then removed using a direct stream of nitrogen prior to vacuum desiccation for a minimum of 4 h. The giant vesicles were formed upon the addition of 3 mL DI H₂O to dried film and were incubated in a 60 °C water bath for 24 h.

2.4. Preparation of Nanometer-Sized Vesicles

Nanometer-sized vesicles were prepared using the film hydration technique.⁴³ Stock solutions of PEG-PBD and PEG-PPO-PEG in chloroform were mixed in the following molar ratios: PEG-PBD/ PEG-PPO-PEG (100:0), PEG-PBD/ PEG-PPO-PEG (95:5), PEG-PBD/ PEG-PPO-PEG (90:10), and PEG-PBD/ PEG-PPO-PEG (75:25). The total amount of PEG-PBD for each of the vesicle compositions was 10 mg. The solvent was removed using a direct stream of nitrogen prior to vacuum desiccation for a minimum of 4 h. An aqueous solution (10 mM HEPES, pH 7.4) was added to dried PEG-PBD film with PEG-PPO-PEG or without PEG-PPO-PEG. The samples were incubated in a 60 °C water bath for 0.5 h and then sonicated for another 0.5 h at the same temperature. Samples were subjected to 10 freeze–thaw–vortex cycles in liquid nitrogen and warm H₂O (60 °C), followed by extrusion 21 times through two stacked 100 nm Nuclepore polycarbonate filters using a stainless steel extruder (Avanti Polar Lipids).

For dye encapsulation, 1 mL of 10 mg/mL SRB, TRITC-dextran (MW 4400), TRITC-dextran (MW 10,000) or TRITC-dextran (MW 40,000) in 10 mM HEPES (pH 7.4) was added to the dried polymer film. For Gd-DTPA-GC encapsulation, 1 mL of 10 mg/mL Gd-DTPA-GC was used. For making ratiometric pH sensors, 1 mL of 10 mM HEPES buffer (pH 7.4) containing 1.5 mg/mL FITC-dextran (MW 59,000–77,000) and 3.5 mg/mL TRITC-dextran (MW 10,000) was used. Freeze-thaw and extrusion were performed as described above. Nonentrapped compounds were removed via size exclusion chromatography using Sepharose CL-4B (Sigma-Aldrich) and rehydration buffer as the eluent.

2.5. Ratiometric pH measurement

For ratiometric pH measurements, 10 mM HEPES buffer solution was prepared with pH values ranging from 5.0 to 8.0 in 0.5 unit increments. Each nanoparticle formulation was diluted to a final PEG-PBD concentration of 10 µg/mL in the buffer at each pH. Solutions were excited at 490 nm and emission collected between 495 and 650 nm.

2.6. In vitro cytotoxicity

The human fibrosarcoma cell line HT1080 (ATCC) was cultured and maintained in Dulbecco's Modified Eagle Medium (DMEM) containing 10% fetal bovine serum (FBS), supplemented with 100 U mL⁻¹ penicillin and 100 U mL⁻¹ streptomycin at 37 °C with 5% CO₂. The cytotoxicity of vesicles with or without Gd-GC was evaluated with MTT assay using HT1080 cells. Briefly, the cells harvested in a logarithmic growth phase were seeded in 96-well plates at $\sim 1 \times 10^4$ cells per well in 100 µL complete DMEM, and incubated at 37 °C in 5% CO₂ atmosphere for 24 h. After removing culture medium, vesicles or Gd-GC loaded vesicles diluted in complete DMEM (100 µL) were added to cell wells at various concentrations. After 24 h treatment, the culture medium was then removed and the cells

were washed with PBS three times. Then 200 μL of DMEM and 20 μL of 5 mg mL^{-1} MTT assays stock solution in PBS were added. After incubating the cells for 4 h, the medium containing unreacted MTT was removed carefully. The obtained blue formazan crystals were dissolved in 150 μL per well DMSO. The absorbance of the solution was measured on a Tecan plate reader (Tecan) at 490 nm. Cell viability (%) was calculated based on the following equation: $(A_{\text{sample}}/A_{\text{control}}) \times 100\%$, where A_{sample} and A_{control} denote absorbencies of the sample well and control well, respectively.

2.7. Instrumentation

Dynamic light scattering (DLS) measurements were performed on a Zetasizer Nano from Malvern Instruments. Fluorescence spectra measurements were done on a SPEX FluoroMax-3 spectrofluorometer (Horiba Jobin Yvon). T_1 relaxation times were determined using a Bruker mq60 MR relaxometer operating at 1.41 T (60 MHz). Gadolinium concentration in samples was determined by ICP-OES analysis using a Genesis ICP-OES (Spectro Analytical Instruments GMBH; Kleve, Germany). Cryogenic Transmission Electron Microscopy (Cryo-TEM) was performed at the University of Pennsylvania in the Nanoscale Characterization Facility (Philadelphia, PA).

3. Results

3.1. Evidence of forming PEG-PBD/PEG-PPO-PEG vesicles

Porous vesicles were produced from the aqueous assembly of the diblock copolymer, PEG-PBD and the triblock copolymer PEG-PPO-PEG. PEG-PPO-PEG was incorporated into the vesicles at 0, 10, or 25mol%. The formation of vesicles was confirmed by preparing micrometer-sized giant vesicles, which were readily observed by light microscopy (Fig. 1). All of the vesicles were spherical in shape; however, the 25mol% PEG-PPO-PEG doped vesicles were smaller in size than vesicles formed from pure PEG-PBD or PEG-PBD doped with 10mol% PEG-PPO-PEG. Vesicles could not be formed from pure PEG-PPO-PEG, i.e. no PEG-PBD.

3.2. Nanometer-sized PEG-PBD/PEG-PPO-PEG vesicles

Nanometer-sized vesicles composed of PEG-PBD and PEG-PPO-PEG were formed by subjecting the micron-sized vesicles, formed via thin film hydration, to multiple freeze-thaw cycles and extrusion through a 100 nm polycarbonate filter. The hydrodynamic diameter of the resulting nanometer-sized vesicles was measured by dynamic light scattering (DLS). DLS presented in Fig. 2 revealed that PEG-PBD vesicles with 10 and 25mol % PEG-PPO-PEG had mean diameters of 121 nm (PDI, 0.114) and 111 nm (PDI, 0.209), respectively, while pure PEG-PBD vesicles had a mean diameter of 120 nm (PDI, 0.231). The slightly smaller size of the 25mol% PEG-PPO-PEG doped vesicles may stem from the interplay between PEG-PBD and PEG-PPO-PEG when more PEG-PPO-PEG was present. In all cases, the DLS measurements revealed a low polydispersity (<0.25 , Table S1, Supporting Information). The morphologies of nano-sized vesicles were further confirmed by cryo-TEM (Fig. S2, Supporting Information). TEM images clearly showed the vesicular structure of PEG-PPO-PEG doped vesicles. To evaluate the stability of PEG-PBD/PEG-PPO-PEG vesicles, the hydrodynamic diameter of the vesicles was measured by DLS for one week

following suspension in HEPES buffer (10 mM, pH 7.4). It was found that PEG-PBD vesicles prepared with 10 and 25mol % PEG-PPO-PEG did not exhibit any significant change in hydrodynamic diameter over this time frame (Fig. S1, Table S1, Supporting Information), indicating that the porous vesicles could be further explored for biomedical applications.

3.3. Membrane Leakage

To investigate whether the polymeric vesicles doped with 0 to 25mol % PEG-PPO-PEG possessed a porous outer membrane, a small fluorescent dye, sulforhodamine B (SRB), was encapsulated within the aqueous interior. Following a 24 h incubation in 10 mM HEPES buffer, the vesicles were centrifuged on a Microcon centrifugal filtering device with a molecular weight cutoff of 100 kDa. The liquid that flowed through the filter was then tested for fluorescence. It was hypothesized that if the vesicles contained pores that were larger than the molecular size of the encapsulated SRB, the encapsulated SRB would diffuse across the membrane bilayer and pass through the filter during centrifugation. Alternatively, if small or no pores were present, no fluorescence would be detected in the flow-through because the encapsulated SRB would remain entrapped within the vesicles, which are too large to pass through the filter. For comparison, the unfiltered vesicles were also measured for fluorescence.

As shown in Fig. 3A, when small SRB was encapsulated within vesicles doped with 25mol % PEG-PPO-PEG, the fluorescence signal detected in the flow-through was very close to that of unfiltered vesicles. When analogous studies were performed on polymersomes that had been doped with 0, 5 or 10mol % PEG-PPO-PEG, the fluorescence signal detected in the flow-through was much lower than that of unfiltered vesicles. Quantitative fluorescence analysis showed that more than 96% of the encapsulated SRB was released within 24 h from vesicles doped with 25mol% PEG-PPO-PEG (Fig. 3B). In contrast, only ~10% of the encapsulated SRB was released from vesicles doped with 10mol% PEG-PPO-PEG and less than 5% leakage was observed from vesicles doped with 0 mol % or 5mol% PEG-PPO-PEG. These results demonstrate that PEG-PPO-PEG can alter the membrane permeability of polymersomes.

3.4. Membrane Retention

To further investigate the porosity of vesicles doped with 25 mol% PEG-PPO-PEG, fluorescently (TRITC)-labeled dextrans with different molecular weights (4.4, 10, and 40 kDa) were encapsulated within the vesicle lumen. The same dextrans were also encapsulated within vesicles composed of 100% PEG-PBD, for comparison (Fig. S3, Supporting Information). Following a 24 h incubation in 10 mM HEPES buffer, the samples were centrifuged on a centrifugal filtering device and the fluorescence of the flow-through was measured. For vesicles doped with 25mol% PEG-PPO-PEG, only the 4.4 kDa dextran exhibited a high level of vesicle leakage (Fig. 4A). In contrast, the 10 kDa and 40 kDa dextrans were largely retained within the vesicle lumen. Quantitative analysis of the fluorescence signals showed that ~50% of the 4.4 kDa dextran was able to escape from vesicles doped with 25 mol% PEG-PPO-PEG, while less than 10% of the 10 kDa dextran and less than 5% of the 40 kDa dextran were able to escape (Fig. 4B). Little to no leakage of

the various dextrans (<5%) was observed for vesicles composed of 100% PEG-PBD. Based on these results and our previous work,⁴⁶ the vesicles doped with 25mol% PEG-PPO-PEG have a pore size of roughly 5 nm in diameter.

3.5. MR Contrast Agents

Gd-based MR contrast agents have relied on the shortening the longitudinal relaxation time (T_1) of surrounding water protons. Prior to demonstrating the feasibility of utilizing porous vesicles to prepare highly efficient MR contrast agents, the permeability of porous vesicles to proton (H^+) was evaluated. Here, a pH-sensitive dye (FITC) and a pH-insensitive reference dye (TRITC) were co-encapsulated into the aqueous interior of vesicles doped with 25mol% PEG-PPO-PEG. To prevent leakage of the small dyes, FITC-dextran (MW 59,000–77,000) and TRITC-dextran (MW 10,000), were used. FITC-dextran and TRITC-dextran were also co-encapsulated into vesicles composed of 100% PEG-PBD, for comparison (Fig. S4, Supporting Information). Both vesicle formulations were suspended in 10 mM HEPES buffer with pH values ranging from 5.0 to 8. As seen in Fig. 5A, the intensity of FITC fluorescence in vesicles doped with 25mol% PEG-PPO-PEG exhibited clear pH dependence, with fluorescence increasing with pH. In contrast, when FITC-dextran was encapsulated within vesicles composed of 100% PEG-PBD, the FITC fluorescence was far less sensitive to changes in pH (Fig. S4). Quantitative analysis of the FITC signal normalized to the TRITC signal is shown in Fig. 5B. These findings suggest that protons are far more efficient at traversing bilayer membranes doped with 25mol% PEG-PPO-PEG.

To prepare highly efficient MR contrast agents, chelated Gd was encapsulated within the interior of vesicles doped with 25mol% PEG-PPO-PEG. To prevent the leakage of small Gd-chelates (i.e. Gd-DTPA, MW 938) through the porous membrane, the Gd-chelates were attached to glycol chitosan, GC (10 to 30 kDa), prior to encapsulation. Attachment of Gd to GC led to an increase in r_1 relaxivity from 3.9 to 11.8 $mM^{-1}s^{-1}$ per Gd, due to the slower molecular rotation of this complex, compared with Gd-DTPA alone (Fig. S5, Supporting Information).³⁴ The r_1 relaxivity of Gd-GC following encapsulation within the porous vesicles was 10.3 $mM^{-1}s^{-1}$ per Gd (Fig. 6A), which was very similar to that of Gd-GC prior to encapsulation. This indicates that Gd-DTPA-GC encapsulated within the porous vesicles experiences a fast water exchange rate with surrounding bulk water, due to the ability of water to pass freely through the porous structure. It should be noted that similar r_1 between Gd-GC-porous vesicle and Gd-GC could be due to a large amount of internal motion within the porous vesicles since Gd-GC were physically encapsulated into aqueous interior of vesicles. In contrast, when Gd-DTPA-GC was encapsulated within non-porous vesicles composed of 100% PEG-PBD, the r_1 was reduced to 7.1 $mM^{-1}s^{-1}$ per Gd (Fig. 6B), which is indicative of poorer water exchange.

The porous polymersome developed here could provide a unique nanoplatfrom for making a highly efficient MR contrast agent. Based on our previous studies and theoretical calculations, up to tens to hundreds of thousands of Gd can be encapsulated within a single ~100 nm vesicle.^{19, 34} The combination of high membrane permeability and high Gd loading capacity of these porous vesicles could result in a high r_1 relaxivity per nanovesicle,⁴⁷ which improves contrast-to-noise, and could enable probing of the molecular

profile of cancer cells for their early detection. Furthermore, this design, i.e. loading Gd within the intra-vesicular volume, is also highly motivated by allowing the porous polymersomes to maintain an unobstructed outer surface that can be used for the highly efficient attachment of cancer targeting ligands.

3.6. Cytotoxicity of porous vesicles

To assess the cytotoxicity of the empty porous vesicles, i.e. no Gd-GC encapsulation, various concentrations of the vesicles were first incubated with HT1080 cells and the metabolic activity of the cells was measured via an MTT (3-(4,5-dimethylthiazol-2-yl)-2,5-diphenyltetrazolium bromide) assay. The data shown in Fig. 7A indicate the cell viabilities normalized to a control cell sample that was not incubated with any polymersomes. For comparison, HT1080 cells were also incubated with nonporous vesicles (i.e. 100 % PEG-PBD). As shown in Fig. 7A, HT1080 cells maintained a viability of over 90% after 24 h incubation with porous vesicles, even at high dosages (0.5 mg/mL). Therefore, the porous vesicles did not seem to have any significant effect on the viability of HT1080 cells. Additionally, the viabilities of HT1080 cells incubated with GC-Gd loaded vesicles at various Gd concentrations were also evaluated after 24 h. As shown in Fig. 7B, cell viabilities are over 90% even at 300 μM of Gd^{3+} for 24 hours, indicating the porous paramagnetic vesicles could be used for in vivo biomedical applications.

4. Discussion

Polymersomes are often made using amphiphilic synthetic polymers including diblock or triblock copolymers. Compared to most natural or synthetic phospholipids, which usually have a molecular weight below 1,000 Da, the synthetic amphiphiles used to form polymersomes can have much larger molecular weights, ranging from several thousand to tens of thousands of Da.⁴⁸ The membrane thickness of the polymersomes increases with increasing molecular weight of amphiphilic polymers. Therefore, the polymersome membrane is significantly thicker (~9–22 nm) than those of liposomes composed of natural phospholipids (3–4 nm).^{16, 49} One significant benefit of the thick membrane of polymersomes is that large amounts of lipophilic drugs can be incorporated, leading to high drug loading capacity. However, the thick membrane of the polymersomes results in lower permeability. This has an impact on some practical applications of polymersomes, since many biomedical applications require that polymersomes release their encapsulants or require that the encapsulants have access to agents in the external environment. For example, therapeutic enzymes can be loaded into the aqueous interior of polymersomes and therefore be protected against a hostile environment.⁵⁰ The effectiveness and utility of the enzyme-encapsulated polymersomes is achieved only if the substrate or the enzymatic reaction product has free entrance or exit through the porous membrane of the polymersomes. Thus, there is a clear need to develop polymersomes with enhanced membrane permeability, which would thus extend their potential applications, such as enzyme/prodrug-based therapy, bioreactors, artificial cells, or bioimaging probes.²³

To date, numerous methods have been explored to alter membrane permeability of polymersomes. For example, Liu and coworkers have developed a method by employing a

light-regulated crosslinking strategy.⁵¹ In brief, amphiphilic block copolymers were synthesized with the hydrophobic block containing photolabile carbamate-caged primary amine moieties. After forming polymersomes, UV light was used to irradiate the sample, which degraded the carbamates and released primary amine moieties that reacted immediately with nearby esters in the membrane. This led to a bilayer hydrophobicity-to-hydrophilicity transition and membrane permeabilization. However, this method requires multi-step synthesis of amphiphilic copolymers. Additionally, this method requires crosslinking with short wavelength UV light, which has the potential to damage encapsulated molecules such as protein or enzyme. Other permeabilization methods often suffer from similar shortcomings, including destabilization of the polymersome, complexity, and cost.

PEG-PPO-PEG is a commercially available (sold as Pluronics) and widely used class of amphiphilic materials with different biological applications. For example, micelles from PEG-PPO-PEG block copolymers can be used as nanocontainers for solubilization of a poorly water soluble drugs.⁵² Many studies have shown that the incorporation of PEG-PPO-PEG into phospholipid bilayers leads to enhanced membrane fluidity and possibly creates channels or pores in the bilayer.^{53–56} However, to our knowledge, little work has been done to study the interaction between PEG-PPO-PEG and polymersome membranes. In this work, different amounts of PEG-PPO-PEG was incorporated into PEG-PBD polymersomes during sample preparation. As shown in Fig. 1, the hybrid PEG-PPO-PEG/PEG-PBD vesicles were formed using a molar ratio of up to 25% PEG-PPO-PEG-to PEG-PBD. Furthermore, nanometer-sized hybrid vesicles were obtained with extrusion techniques, which are widely used to control the size of phospholipid liposomes.

The leakage and retention properties of PEG-PPO-PEG/PEG-PBD vesicles were studied using different membrane compositions or encapsulants with different molecular weights. As shown in Fig. 3, significant SRB was released from the 25mol% PEG-PPO-PEG/75mol % PEG-PBD vesicles. On the other hand, large molecules, such as 10K dextran, were well retained inside of the PEG-PPO-PEG/PEG-PBD vesicles. These findings clearly demonstrated that PEG-PPO-PEG was able to tune permeability of polymersome membranes, similar to that of phospholipid membranes.³⁵ Unlike many other methods for creating porous polymersomes, which often involve complicated processes, the method presented herein has some important advantages: (i) it is an easy, one-step method as it does not include any synthesis and purification; (ii) it is a cost-efficient method as it does not include the use of any expensive materials; (iii) it is a green method as it does not include the use of any toxic materials or the generation of any toxic by-products. Therefore, we believe the method presented in this work can potentially extend the application of polymersomes.

5. Conclusion

In this work we reported a simple method to tune the permeability of polymersomes. The enhanced membrane permeability was simply achieved by incorporation of appropriate amounts of the triblock copolymer PEG-PPO-PEG into polymersome membranes. The porous vesicles can retain large molecules, while small molecules can easily diffuse through

the porous membrane. Highly efficient MR contrast agents have been developed to demonstrate a representative biomedical application. It is envisioned that the porous polymersomes made from the current method can significantly extend the application of polymersomes, ranging from drug delivery to molecular imaging to nanofactories.

Supplementary Material

Refer to Web version on PubMed Central for supplementary material.

Acknowledgements

This work was supported in part by the National Institutes of Health NCI R01CA175480 (ZC) and R01CA157766 (AT).

References

1. Discher DE, Eisenberg A. *Science*. 2002; 297:967–973. [PubMed: 12169723]
2. Anajafi T, Mallik S. *Ther Deliv*. 2015; 6:521–534. [PubMed: 25996048]
3. Jeong IK, Gao GH, Li Y, Kang SW, Lee DS. *Macromol Biosci*. 2013; 13:946–953. [PubMed: 23696500]
4. Kim MS, Lee DS. *Chem Commun (Camb)*. 2010; 46:4481–4483. [PubMed: 20461280]
5. Surovtseva EV, Johnston AH, Zhang W, Zhang Y, Kim A, Murakoshi M, Wada H, Newman TA, Zou J, Pyykko I. *Int J Pharm*. 2012; 424:121–127. [PubMed: 22227343]
6. Cheng Z, Thorek DL, Tsourkas A. *Adv Funct Mater*. 2009; 19:3753–3759. [PubMed: 23293575]
7. Cheng Z, Tsourkas A. *Langmuir*. 2008; 24:8169–8173. [PubMed: 18570445]
8. Pourtau L, Oliveira H, Thevenot J, Wan Y, Brisson AR, Sandre O, Miraux S, Thiaudiere E, Lecommandoux S. *Adv Healthc Mater*. 2013; 2:1420–1424. [PubMed: 23606565]
9. Sanson C, Diou O, Thevenot J, Ibarboure E, Soum A, Brulet A, Miraux S, Thiaudiere E, Tan S, Brisson A, Dupuis V, Sandre O, Lecommandoux S. *ACS Nano*. 2011; 5:1122–1140. [PubMed: 21218795]
10. Cheng Z, Al Zaki A, Jones IW, Hall HK Jr, Aspinwall CA, Tsourkas A. *Chem Commun (Camb)*. 2014; 50:2502–2504. [PubMed: 24457826]
11. Yang X, Grailer JJ, Rowland IJ, Javadi A, Hurley SA, Matson VZ, Steeber DA, Gong S. *ACS Nano*. 2010; 4:6805–6817. [PubMed: 20958084]
12. Bleul R, Thiermann R, Marten GU, House MJ, St Pierre TG, Hafeli UO, Maskos M. *Nanoscale*. 2013; 5:11385–11393. [PubMed: 23820598]
13. Kokuryo D, Anraku Y, Kishimura A, Tanaka S, Kano MR, Kershaw J, Nishiyama N, Saga T, Aoki I, Kataoka K. *J Control Release*. 2013; 169:220–227. [PubMed: 23542239]
14. Yang X, Grailer JJ, Rowland IJ, Javadi A, Hurley SA, Steeber DA, Gong S. *Biomaterials*. 2010; 31:9065–9073. [PubMed: 20828811]
15. Ahmed F, Pakunlu RI, Brannan A, Bates F, Minko T, Discher DE. *Journal of Controlled Release*. 2006; 116:150–158. [PubMed: 16942814]
16. Ghoroghchian PP, Frail PR, Susumu K, Blessington D, Brannan AK, Bates FS, Chance B, Hammer DA, Therien MJ. *P Natl Acad Sci USA*. 2005; 102:2922–2927.
17. Robbins GP, Jimbo M, Swift J, Therien MJ, Hammer DA, Dmochowski IJ. *Journal of the American Chemical Society*. 2009; 131:3872–3874. [PubMed: 19249827]
18. Le Meins JF, Sandre O, Lecommandoux S. *Eur Phys J E*. 2011; 34
19. Cheng ZL, Thorek DLJ, Tsourkas A. *Adv Funct Mater*. 2009; 19:3753–3759. [PubMed: 23293575]
20. Nardin C, Widmer J, Winterhalter M, Meier W. *Eur Phys J E*. 2001; 4:403–410.
21. Kim MS, Lee DS. *Chem Commun*. 2010; 46:4481–4483.

22. Kim KT, Cornelissen JJLM, Nolte RJM, van Hest JCM. *Adv Mater.* 2009; 21:2787-+.
23. Gaitzsch J, Appelhans D, Wang LG, Battaglia G, Voit B. *Angew Chem Int Edit.* 2012; 51:4448–4451.
24. Yan Q, Wang JB, Yin YW, Yuan JY. *Angew Chem Int Edit.* 2013; 52:5070–5073.
25. Oh KT, Yin HQ, Lee ES, Bae YH. *J Mater Chem.* 2007; 17:3987–4001.
26. Wang YP, Ma N, Wang ZQ, Zhang X. *Angew Chem Int Edit.* 2007; 46:2823–2826.
27. Lecommandoux SB, Sandre O, Checot F, Rodriguez-Hernandez J, Perzynski R. *Adv Mater.* 2005; 17:712-+.
28. Kamat NP, Katz JS, Hammer DA. *J Phys Chem Lett.* 2011; 2:1612–1623. [PubMed: 22110844]
29. Nallani M, Benito S, Onaca O, Graff A, Lindemann M, Winterhalter M, Meier W, Schwaneberg U. *J Biotechnol.* 2006; 123:50–59. [PubMed: 16364484]
30. Graff A, Fraysse-Ailhas C, Palivan CG, Grzelakowski M, Friedrich T, Vebert C, Gescheidt G, Meier W. *Macromol Chem Phys.* 2010; 211:229–238.
31. Kim AJ, Kaucher MS, Davis KP, Peterca M, Imam MR, Christian NA, Levine DH, Bates FS, Percec V, Hammer DA. *Adv Funct Mater.* 2009; 19:2930–2936.
32. Srinivas G, Discher DE, Klein ML. *Nano Lett.* 2005; 5:2343–2349. [PubMed: 16351175]
33. Discher DE, Ortiz V, Srinivas G, Klein ML, Kim Y, David CA, Cai SS, Photos P, Ahmed F. *Prog Polym Sci.* 2007; 32:838–857. [PubMed: 24692840]
34. Cheng ZL, Tsourkas A. *Langmuir.* 2008; 24:8169–8173. [PubMed: 18570445]
35. Johnsson M, Silvander M, Karlsson G, Edwards K. *Langmuir.* 1999; 15:6314–6325.
36. Li F, Ketelaar T, Marcelis ATM, Leermakers FAM, Stuart MAC, Sudholter EJR. *Macromolecules.* 2007; 40:329–333.
37. Schillen K, Bryskhe K, Mel'nikova YS. *Macromolecules.* 1999; 32:6885–6888.
38. Foster T, Dorfman KD, Davis HT. *Langmuir.* 2010; 26:9666–9672. [PubMed: 20380397]
39. Rodriguez-Garcia R, Mell M, Lopez-Montero I, Netzel J, Hellweg T, Monroy F. *Soft Matter.* 2011; 7:1532–1542.
40. Atkin R, De Fina LM, Kiederling U, Warr GG. *J Phys Chem B.* 2009; 113:12201–12213. [PubMed: 19691356]
41. Li F, de Wolf FA, Marcelis ATM, Sudholter EJR, Stuart MAC, Leermakers FAM. *Angew Chem Int Edit.* 2010; 49:9947–9950.
42. Bryskhe K, Jansson J, Topgaard D, Schillen K, Olsson U. *J Phys Chem B.* 2004; 108:9710–9719.
43. Cheng ZL, Elias DR, Kamat NP, Johnston ED, Poloukhine A, Popik V, Hammer DA, Tsourkas A. *Bioconjugate Chem.* 2011; 22:2021–2029.
44. Crayton SH, Tsourkas A. *ACS nano.* 2011; 5:9592–9601. [PubMed: 22035454]
45. Nwe K, Huang CH, Tsourkas A. *J Med Chem.* 2013; 56:7862–7869. [PubMed: 24044414]
46. Muhandiramlage TP, Cheng ZL, Roberts DL, Keogh JP, Hall HK, Aspinwall CA. *Anal Chem.* 2012; 84:9754–9761. [PubMed: 23083108]
47. Huang CH, Tsourkas A. *Curr Top Med Chem.* 2013; 13:411–421. [PubMed: 23432004]
48. Christian DA, Cai S, Bowen DM, Kim Y, Pajerowski JD, Discher DE. *Eur J Pharm Biopharm.* 2009; 71:463–474. [PubMed: 18977437]
49. Won YY, Brannan AK, Davis HT, Bates FS. *J Phys Chem B.* 2002; 106:3354–3364.
50. van Dongen SFM, Verdurmen WPR, Peters RJRW, Nolte RJM, Brock R, van Hest JCM. *Angew Chem Int Edit.* 2010; 49:7213–7216.
51. Wang X, Liu G, Hu J, Zhang G, Liu S. *Angewandte Chemie.* 2014; 53:3138–3142. [PubMed: 24519898]
52. Kadam Y, Yerramilli U, Bahadur A, Bahadur P. *Colloids and surfaces. B, Biointerfaces.* 2011; 83:49–57. [PubMed: 21123038]
53. Batrakova E, Lee S, Li S, Venne A, Alakhov V, Kabanov A. *Pharm Res-Dordr.* 1999; 16:1373–1379.
54. Krylova OO, Pohl P. *Biochemistry-US.* 2004; 43:3696–3703.
55. Schulz M, Olubummo A, Binder WH. *Soft Matter.* 2012; 8:4849–4864.

56. Rahman M, Yu E, Forman E, Roberson-Mailloux C, Tung J, Tringe J, Stroeve P. Colloid Surface B. 2014; 122:818–822.

Author Manuscript

Author Manuscript

Author Manuscript

Author Manuscript

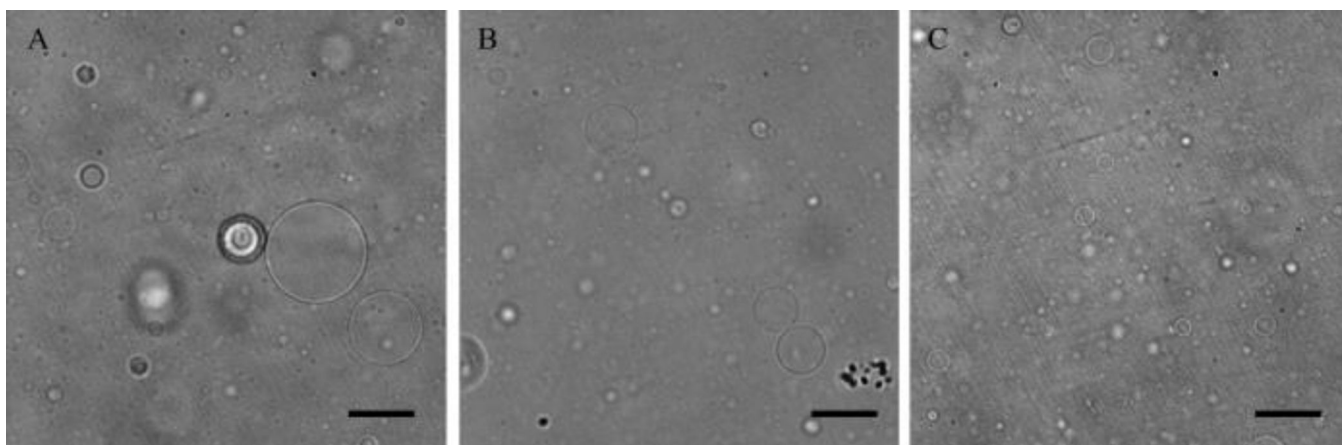


Fig. 1.

Optical images of giant vesicles composed of PEG-PBD and PEG-PPO-PEG at three different molar ratios. (A) 100% PEG-PBD, (B) 90mol% PEG-PBD/10mol% PEG-PPO-PEG, and (C) 75mol% PEG-PBD/25mol% PEG-PPO-PEG. All vesicles were formed by the film hydration method. Scale bar: 50 μm .

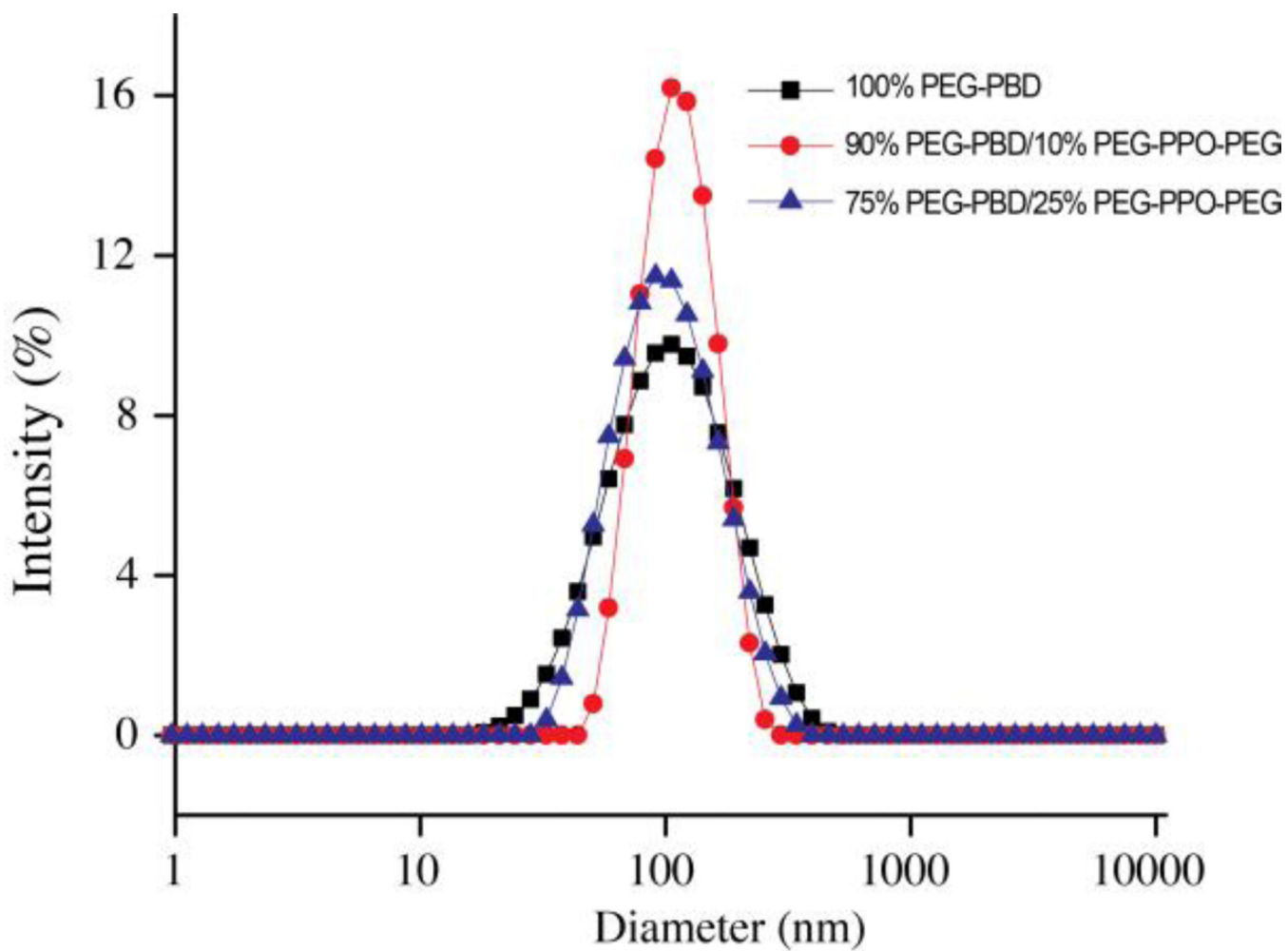
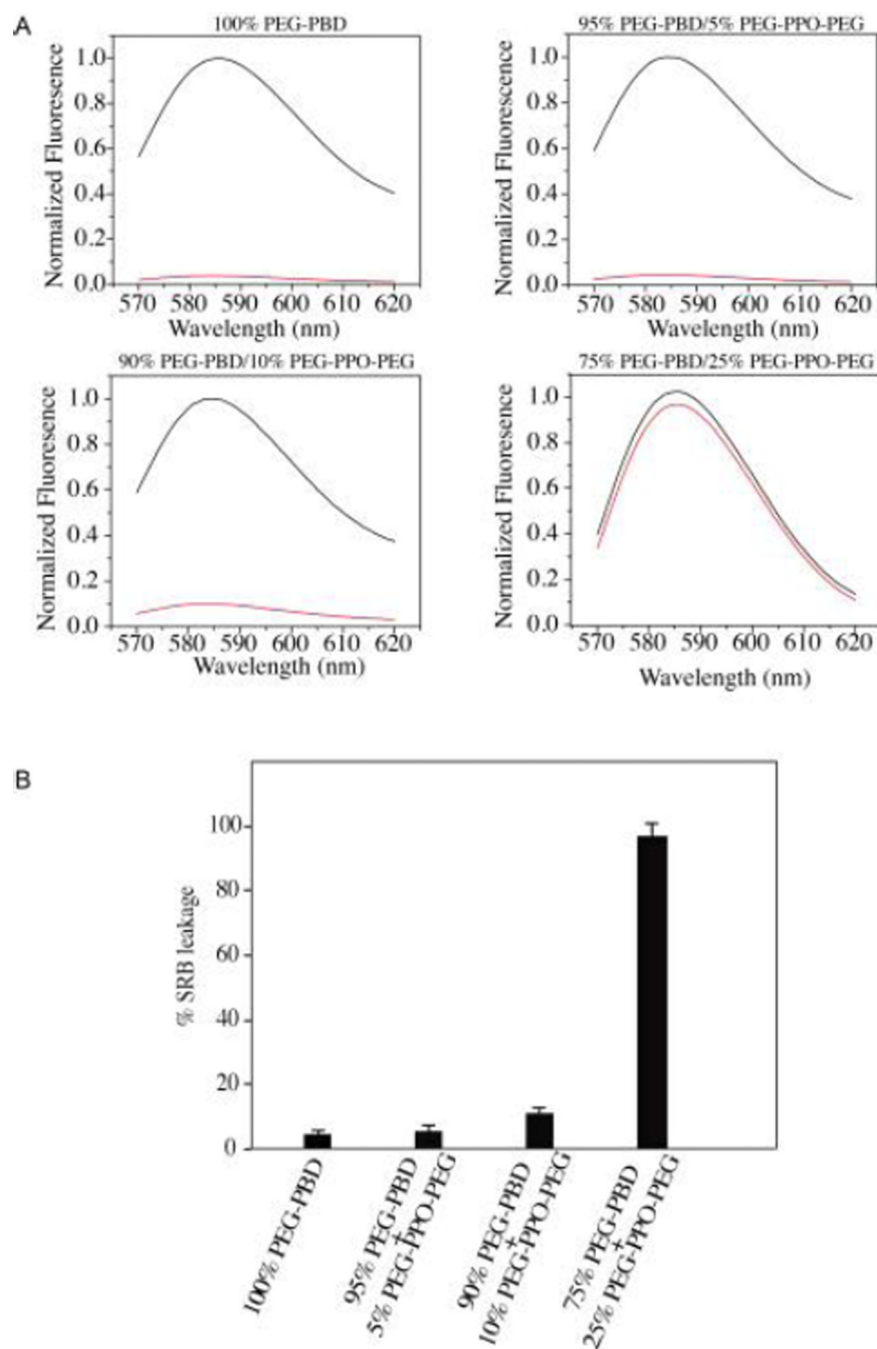


Fig. 2. Intensity-weighted hydrodynamic diameter measurement of nanometer-sized vesicles composed of PEG-PBD and PEG-PPO-PEG at three different molar ratios.

**Fig. 3.**

(A) Release of encapsulated SRB from polymeric vesicles prepared with 100mol% PEG-PBD, 95mol% PEG-PBD/5mol% PEG-PPO-PEG, 90mol% PEG-PBD/10mol% PEG-PPO-PEG or 75mol% PEG-PBD/25mol% PEG-PPO-PEG. Following 24 h incubation in HEPES buffer (10mM, pH 7.4), the vesicles were centrifuged on a Microcon filtering device with a 100 KDa MWCO membrane. The liquid that flowed through the filter was measured for fluorescence (red line). The fluorescence of unfiltered sample in the presence of Triton X-100 was also recorded (black line). The fluorescence intensity is normalized relative to

the intensity of unfiltered sample at 585 nm. (B) Quantitative analysis of leakage data from Fig. 3A. The percent leakage of encapsulated SRB was calculated as $(I_a/I_b) \times 100$, where I_a is the fluorescence intensity at emission wavelength 585 nm for the liquid that flowed through the filter, and I_b is the fluorescence intensity at emission wavelength 585 nm for the unfiltered sample.

Author Manuscript

Author Manuscript

Author Manuscript

Author Manuscript

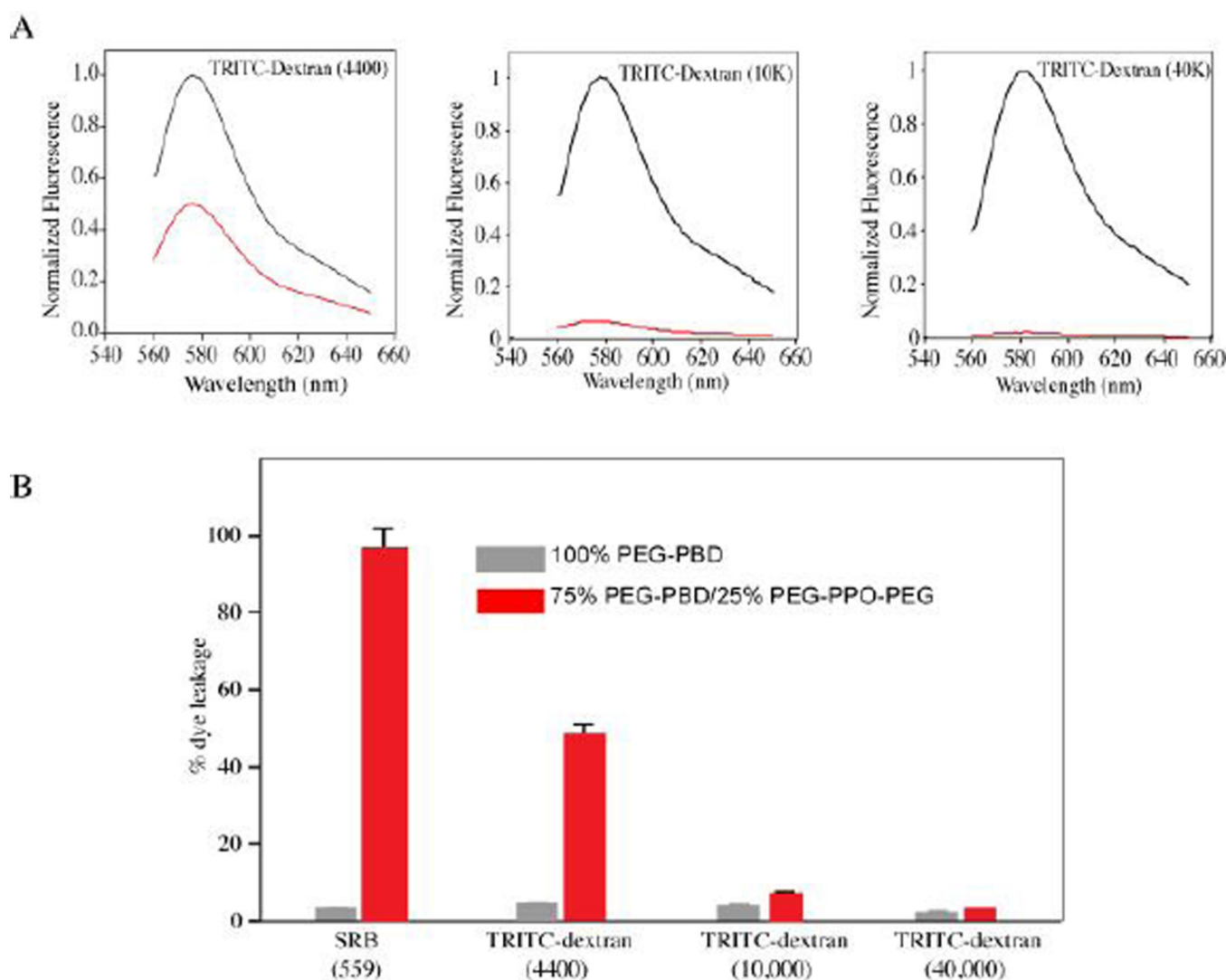


Fig. 4. (A) Release and retention of encapsulated compounds including TRITC-dextran (4,400), TRITC-dextran (10 K) and TRITC-dextran (40 K) within the polymeric vesicles. Vesicles were prepared with 75mol% PEG-PBD/25mol% PEG-PPO-PEG. Following 24 h incubation in HEPES buffer (10 mM, pH 7.4), the vesicles were centrifuged on a Microcon filtering device with a 100 KDa MWCO membrane. The liquid that flowed through the filter was measured for fluorescence (red line). The fluorescence of unfiltered sample in the presence of Triton X-100 was also recorded (black line). The fluorescence intensity is normalized relative to the intensity of unfiltered sample at 585 nm. (B) Quantitative analysis of leakage and retention data from Fig. 4A. The percent leakage of encapsulated compounds was calculated as $(I_a/I_b) \times 100$, where I_a is the fluorescence intensity at emission wavelength 585 nm for the liquid that flowed through the filter, and I_b is the fluorescence intensity at emission wavelength 585 nm for the unfiltered sample. For comparison, the data of SRB leakage from vesicles of 100 % PEG-PBD or 75mol% PEG-PBD/25mol% PEG-PPO-PEG was also included in the Figure.

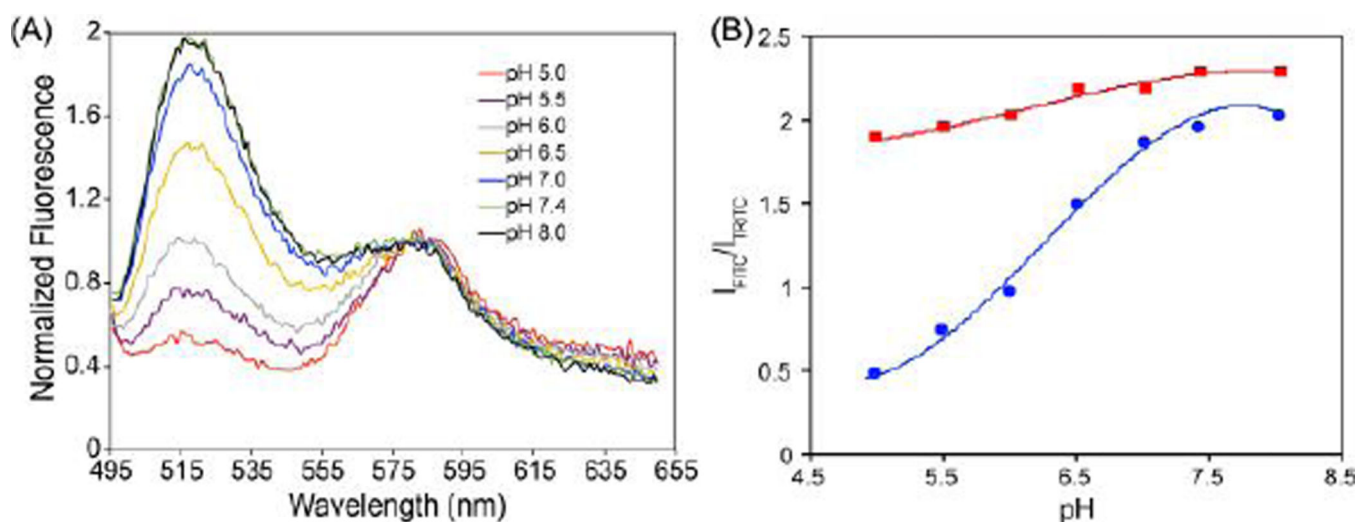


Fig. 5.

(A) Sensitivity of FITC-dextran (MW: 59,000–77,000) encapsulated within 75mol% PEG-PBD/25mol% PEG-PPO-PEG vesicles to pH. For ratiometric measurements, the reference dye TRITC-dextran (MW: 10,000) was also co-loaded with FITC-dextran into the aqueous interior of 75mol% PEG-PBD/25mol% PEG-PPO-PEG vesicles. (B) Fluorescence emission wavelength ratiometric plots for 75mol% PEG-PBD/25mol% PEG-PPO-PEG vesicles (●) and 100mol% PEG-PBD vesicles (■) based on the I_{FITC}/I_{TRITC} in Fig. 5A & Fig. S4.

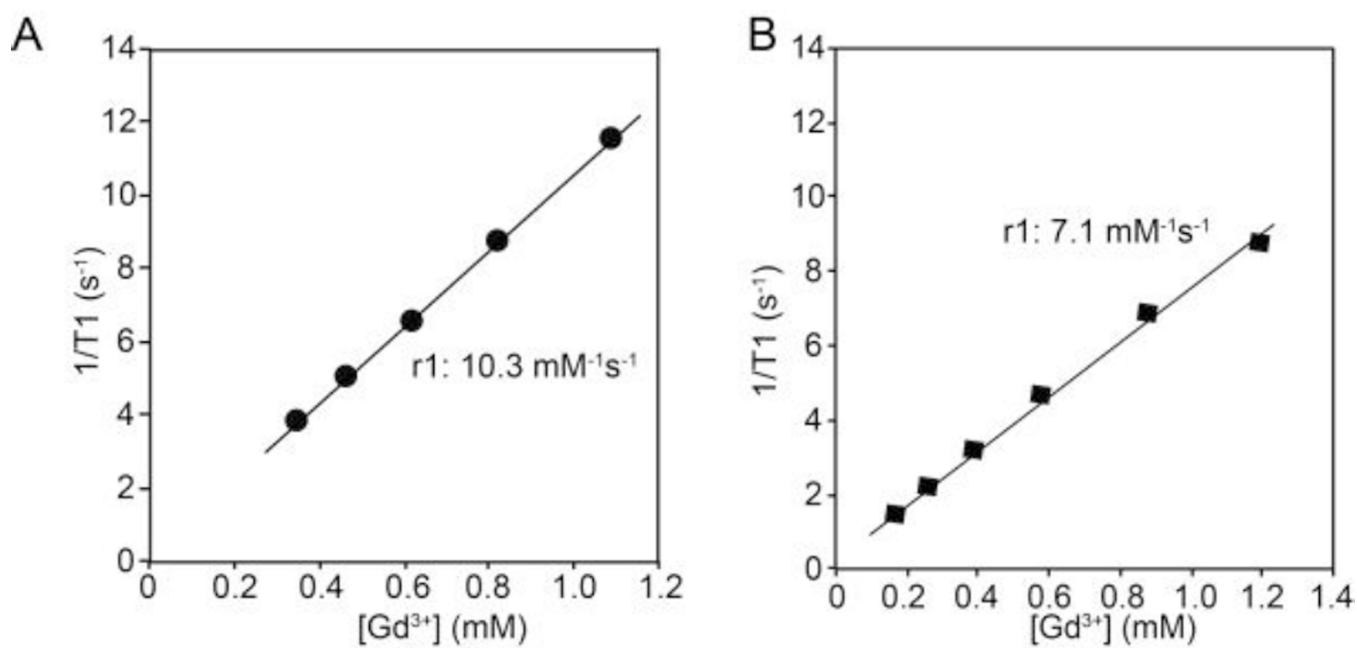


Figure 6. Relaxivity determination for Gd-GC conjugates encapsulated within vesicles composed of 75mol% PEG-PBD/25mol% PEG-PPO-PEG (A). Comparisons are made to Gd-GC conjugates encapsulated within 100mol% PEG-PBD vesicles (B).

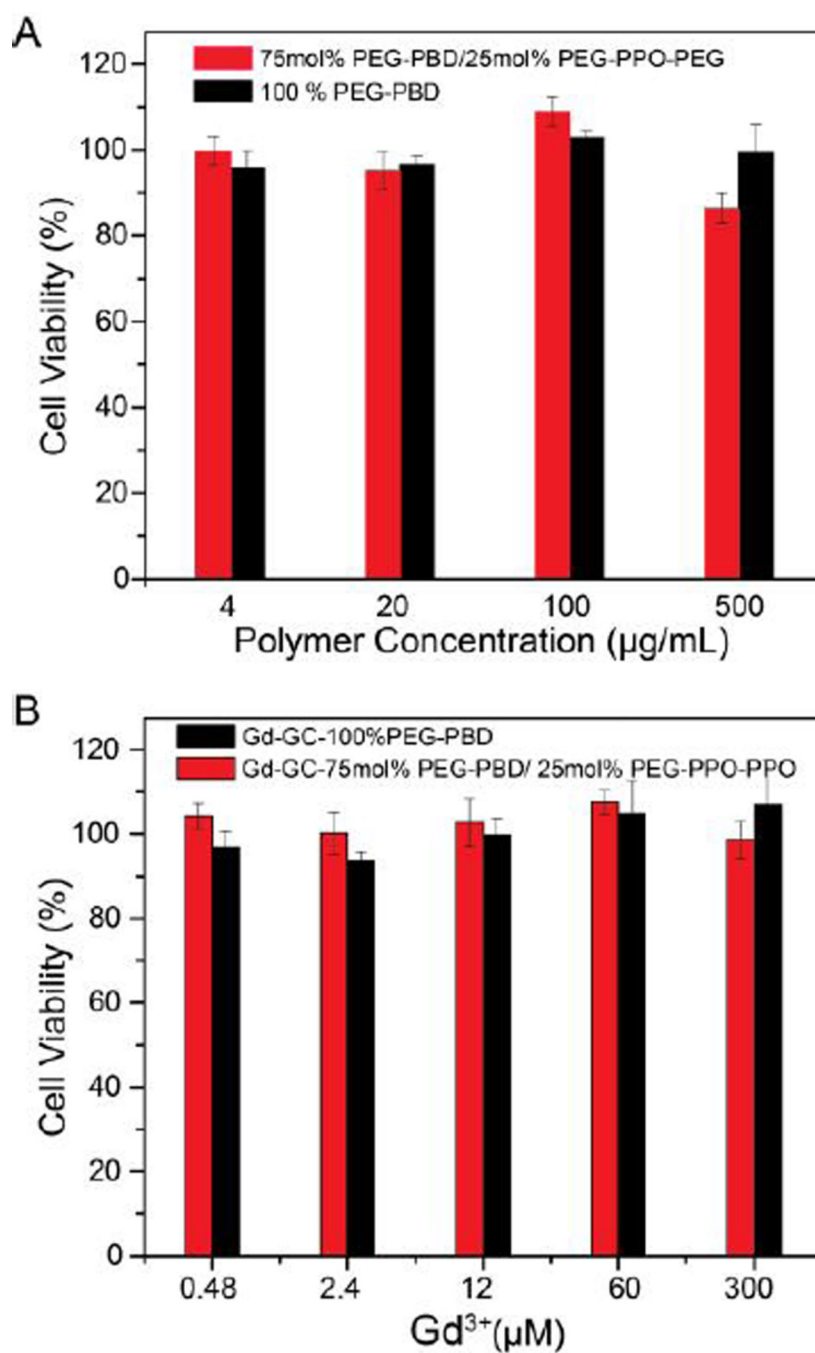


Fig. 7. Cell viability of HT1080 cells after incubation with (A) empty vesicles and (B) Gd-GC conjugates encapsulated vesicles for 24 h at 37 °C. For comparison, HT 1080 cells were also incubated with 100% PEG-PBD vesicles with and without Gd-GC encapsulation. Data are presented as the average \pm standard deviation (n=4).